Geochemical Results from Strain-Meter Boreholes Drilled in Yellowstone National Park – Final Report

Richard M Conrey*

Peter Hooper GeoAnalytical Laboratory
School of the Environment
Washington State University
Pullman, WA 99164-2812

March 29, 2014

* geolab@mail.wsu.edu or 509-335-1626

This report describes the results of analytical work conducted at the WSU Peter Hooper GeoAnalytical Laboratory under the auspices of CESU agreement H1200090004 during the period 2010 to 2014. Cuttings from strain-meter boreholes drilled at Yellowstone National Park (YNP) were chemically analyzed using methods developed at WSU for rock analysis. Eighty five samples were analyzed in total using X-Ray Fluorescence (XRF) and Inductively Coupled Plasma – Mass Spectrometry (ICP-MS). Simple gravimetry was used to measure volatile loss (loss on ignition or LOI) at 900°C. Samples were provided as chips by Cheryl Jaworowski of YNP.

Sample Treatment and Methods

Approximately 50-100 grams of chips were received as single samples. Because the chips had already been treated and selected by Cheryl Jaworowski no further treatment was undertaken; samples were simply ground in entirety in a tungsten carbide (WC) ring-mill to fine (sub 20 micron) powder for analysis.

Briefly, the method employed for elemental determinations by XRF at WSU is as follows. 3.5 grams of powdered sample are weighed and mixed with 7.0 grams of Lithium tetraborate and fused in graphite crucibles in a muffle furnace at 1000°C for approximately 45 minutes (see Johnson et al., 1999, available on-line at http://environment.wsu.edu/facilities/geolab/technotes/xrf_method.html). The fused pellet is ground to powder in a WC ring-mill and re-fused at the same temperature for the same length of time. The bottom surface of the doubly ground pellet is flattened with diamond laps down to a 15 micron finish. The flat surface is presented to a powerful X-ray tube and the intensities of the fluoresced characteristic X-rays from each of the 34 analyte elements within the pellet are corrected for spectral interference and the presence of the other major and minor elements. The corrected intensities are compared with the known corrected intensities from approximately 75 to 106 certified reference materials (CRMs). Calibration curves relating corrected intensity to chemical abundance or concentration are re-measured approximately every 8 months and the concentrations of the analyte elements for unknowns are calculated from those curves. Drift of the instrument is monitored almost daily with runs of two CRMs as unknowns. Small drift correction is made for the elements Si, Al, Ti, Fe, and Na as needed.

The method for ICP-MS analysis at WSU is as follows. 2.0 or 3.0 grams of the powdered sample is weighed and mixed with an equal amount of Lithium tetraborate and fused in graphite crucibles in a muffle furnace at 1000°C for approximately 45 minutes. The fused pellet is cleaned and ground to powder in a

a steel ring-mill. The ground fused powder is digested in perchloric and hydrofluoric acids to remove most of the silicon and to dissolve all of the powdered glass. The evaporated solution is re-digested in nitric acid and then heavily diluted before aspiration into the plasma torch. Fuller description of the method and calibration can be found in-line at http://environment.wsu.edu/facilities/geolab/technotes/icp-ms_method.html.

Results

All analytical data for the 85 samples, including XRF, ICP-MS, and LOI determinations, have been reported to Cheryl Jaworowski at YNP and will be available as appendices in her reports (USGS report, in progress).

Repeatability and precision

The precision of the analytical methods used at WSU is inferred statistically from our extensive dataset of repeat experiments from powdered samples. We determine approximately 200 and 100 repeat analyses per year out of approximately 5500 samples analyzed per year for XRF and 2500 samples analyzed per year for ICP-MS, respectively. Our estimated precision for XRF analyses is shown in Table 1, along with the repeated analyses from powder for four of the YNP samples. All of the XRF data is well within the expected uncertainties of our analytical method. Uncertainties for ICP-MS determinations are typically less than 2-4% relative (of the concentration), and again all of these repeat data are well within those uncertainties.

The repeatability of the analytical data from powder does not capture all of the uncertainty associated with these bulk rock analyses. There is uncertainty in sampling and sample selection, which may be considerable in this case because many of the samples are from heterogeneous tuffaceous units. The problem is particularly acute because these high-silica rhyolite rocks contain trace phases of uncommon minerals that comprise a considerable proportion of the budget of some trace elements in the rocks. In this case the mineral chevkinite has been found to be a problem we think due to its very high content of Nb (see below). Other rare earth element (REE) bearing minerals or zircon are also present and may play a significant role. Small differences in the sorting or aggregation of such minerals might skew the analytical determinations of selected elements, especially Nb, but also including the REEs and other trace elements such as Zr and Hf. It seems likely that the sampling errors, especially for the tuffs, overwhelm the small

Table 1. XRF and ICP-MS repeatability.

	Canyon 165-170	Canyon 165-170 R	Norris B205-335	Norris B205-335R	Grant II B944-270	Grant II B944-270R	Madison B207-A	Madison B207-A R	XRF precision
Date	12-Aug-12	14-Aug-12	3-Mar-14	5-Mar-14	4-Mar-14	5-Mar-14	11-Aug-11	12-Aug-11	2 sigma (95%)
	Unnormalized Major Elements (Weight %):								
SiO2	75.32	75.46	75.96	76.50	77.28	76.85	76.39	76.79	0.58
TiO2	0.304	0.304	0.153	0.156	0.163	0.163	0.163	0.164	0.017
Al2O3	11.55	11.59	11.90	12.00	11.86	11.80	11.87	11.89	0.16
FeO*	1.94	1.94	1.74	1.85	1.33	1.35	1.43	1.43	0.20
MnO	0.095	0.095	0.014	0.014	0.028	0.029	0.029	0.029	0.002
MgO	0.03	0.03	0.03	0.07	0.05	0.06	0.04	0.04	0.076
CaO	0.55	0.56	0.36	0.41	0.38	0.38	0.33	0.33	0.064
Na2O	3.11	3.11	3.21	3.25	3.33	3.31	3.31	3.32	0.045
K2O	4.83	4.84	5.05	5.08	5.28	5.25	5.29	5.30	0.031
P2O5	0.034	0.033	0.016	0.018	0.015	0.015	0.011	0.011	0.005
Sum	97.77	97.96	98.44	99.35	99.73	99.21	98.86	99.31	
LOI (%)	0.86	0.86	0.79	0.79	0.52	0.52	0.40	0.40	
	Normalized Major Elements (Weight %):								
SiO2	77.03	77.04	77.16	77.00	77.49	77.46	77.27	77.33	0.19
TiO2	0.311	0.311	0.156	0.157	0.164	0.165	0.165	0.166	0.012
Al2O3	11.82	11.83	12.09	12.08	11.89	11.90	12.01	11.97	0.082
FeO*	1.99	1.98	1.77	1.86	1.34	1.36	1.44	1.44	0.18
MnO	0.097	0.097	0.014	0.014	0.029	0.029	0.029	0.029	0.002
MgO	0.03	0.03	0.03	0.07	0.05	0.06	0.04	0.04	0.073
CaO	0.57	0.57	0.37	0.42	0.38	0.38	0.33	0.33	0.043
Na2O	3.18	3.17	3.26	3.27	3.34	3.34	3.35	3.34	0.036
K2O	4.94	4.94	5.13	5.11	5.29	5.30	5.35	5.34	0.015
P2O5	0.034	0.034	0.016	0.018	0.015	0.015	0.011	0.011	0.003
Total	100.00	100.00	100.00	100.00	100.00	100.00	100.00	100.00	
	Unnormalized Trace Elements (ppm):								
Ni	0	0	2	2	2	3	1	1	3.5
Cr	7	7	5	4	2	3	3	4	3.0
Sc	6	5	2	2	2	3	3	2	1.6
V	4	5	4	5	3	3	2	1	5.0
Ba	904	908	397	398	318	318	252	251	11.7
Rb	153	152	176	177	187	184	193	194	1.7
Sr	56	55	22	25	14	13	11	11	4.6
Zr	330	331	275	277	237	237	232	234	3.9
Y	62	62	58	59	69	69	60	60	1.2
Nb	47.8	47.6	53.9	53.8	49.5	48.9	48.5	49.2	1.2
Ga	21	19	23	22	20	21	20	20	2.7
Cu	4	6	2	5	2	2	2	2	7.4
Zn	64	64	66	64	65	63	53	53	3.3
Pb	34	34	22	23	37	38	29	29	2.6
La	77	74	87	87	89	87	88	86	5.7
Ce	143	143	173	176	160	162	162	164	7.9
Th	24	24	31	31	27	28	27	27	1.6
Nd	60	59	67	67	65	66	64	65	4.3
U	5	6	6	6	6	6	7	6	2.7
Cs	4	6	0	1	4	5			5.1
As >/=			2	3	15	13	19	17	
sum tr.	2003	2007	1475	1489	1374	1372	1275	1278	
in %	0.20	0.20	0.15	0.15	0.14	0.14	0.13	0.13	
sum m+tr	97.97	98.16	98.59	99.50	99.86	99.34	98.98	99.43	
M+Toxides	98.01	98.20	98.62	99.53	99.89	99.37	99.01	99.46	
w/LOI	98.87	99.06	99.41	100.32	100.42	99.90	99.41	99.86	
if Fe3+	99.09	99.27	99.60	100.52	100.56	100.05	99.57	100.02	
ICP-MS data (all in ppm)									
La	77.71	77.74	89.99	89.80	91.01	91.20	91.31	91.80	
Ce	155.34	157.34	180.30	178.55	165.47	166.57	170.78	175.58	
Pr	16.88	17.07	19.21	19.10	19.06	19.11	19.42	19.49	
Nd	61.56	61.37	68.09	67.68	67.01	67.38	68.05	69.01	
Sm	12.79	12.67	13.42	13.42	13.19	13.29	13.37	13.50	
Eu	1.59	1.58	0.96	0.96	0.80	0.81	0.73	0.74	
Gd	11.51	11.40	11.50	11.51	11.80	11.72	11.74	11.69	
Tb	1.96	1.98	1.93	1.94	2.01	2.00	1.97	1.98	
Dy	11.97	12.06	11.51	11.35	12.17	12.14	11.99	12.09	
Ho	2.42	2.42	2.21	2.23	2.46	2.46	2.38	2.38	
Er	6.41	6.45	5.86	5.84	6.68	6.62	6.43	6.45	
Tm	0.93	0.95	0.84	0.82	0.97	0.98	0.94	0.95	
Yb	5.75	5.72	5.07	5.09	6.00	5.91	5.74	5.75	
Lu	0.88	0.87	0.74	0.74	0.86	0.91	0.86	0.85	
Ba	925	924	401	404	322	320	254	255	
Th	24.15	24.18	30.13	29.97	26.75	26.64	27.23	27.10	
Nb	48.67	48.81	52.95	52.61	47.10	47.80	49.73	49.19	
Y	61.28	60.87	55.29	54.93	65.00	65.75	58.34	59.11	
Hf	9.85	9.88	9.35	9.22	8.19	8.09	8.35	8.43	
Ta	3.53	3.51	3.78	3.67	3.39	3.43	3.61	3.56	
U	5.57	5.57	5.74	5.74	6.35	6.23	6.49	6.43	
Pb	33.97	34.20	21.61	21.26	35.38	35.05	27.81	27.52	
Rb	156.5	155.5	173.5	174.2	183.2	184.7	196.8	199.4	
Cs	3.83	3.81	2.11	2.18	5.84	5.73	3.71	3.67	
Sr	59	59	23	23	15	14	11	11	
Sc	5.1	4.8	1.7	1.8	2.1	1.9	3.4	3.4	
Zr	343	342	278	275	233	239	248	257	

analytical errors associated with our methods. This fact should be borne in mind when interpreting the results of these analyses. Most attention should be paid to the drill log and rather less to the analytical data.

Comparison of XRF and ICP-MS results

Many trace element abundances are determined using both of our analytical methods and thus serve as a cross check on consistency and overall analytical uncertainty. Comparisons of the determinations are shown in Figure 1 on the following pages, where the ICP-MS determined abundances are plotted versus the XRF determined concentrations. All scales are in ppm and the best fit lines to the data are shown, along with their statistics.

The overall agreement of these data are good, as evidenced by the uniformly high correlation coefficients, with the exception of the data for U and Cs, where large systematic biases between the two methods can be seen (Figs. 1l and n). Normally we do not see such biases so their presence here is puzzling and worthy of further pursuit within our laboratory. At the low concentration levels in these samples the ICP-MS data should be far superior.

The best agreement is found for the elements Rb, Sr, Th, and Sc (Figs. 1b, c, k, and m), where there are essentially no systematic biases between the two methods, or they are below the 1% level and thus well within the analytical uncertainties of both techniques. Ba (Fig. 1a) is nearly in this category with a slight overall bias of about 2% and an offset of 2.5 ppm, just barely within the analytical uncertainties.

Agreement is less robust for the elements Zr, Y, Pb, La, Ce, and Nd (Figs. 1d, e, g, h, I, and j). These elements show systematic biases of 3.5 to 6.5%, with some significant offsets such as the case of 4 ppm for Zr (Fig. 1d). The primary reason for such bias is likely the different sets of CRMs used to calibrate the two methods. The ICP-MS calibrations employ in-house standards, run conjointly with each batch of samples, that are calibrated to a set of internationally characterized CRMs, whereas the XRF calibrations are based on stable calibrations of a larger set of CRMs. These are fairly small biases, especially considering the common inter-laboratory biases in trace element determinations, but they are outside of our reported analytical uncertainties and thus worthy of further investigation within our laboratory.

Nb presents a special case for these samples, in part due to the systematic offset of 1.3 ppm with no other bias. Nb is also subject to nugget effects in these samples

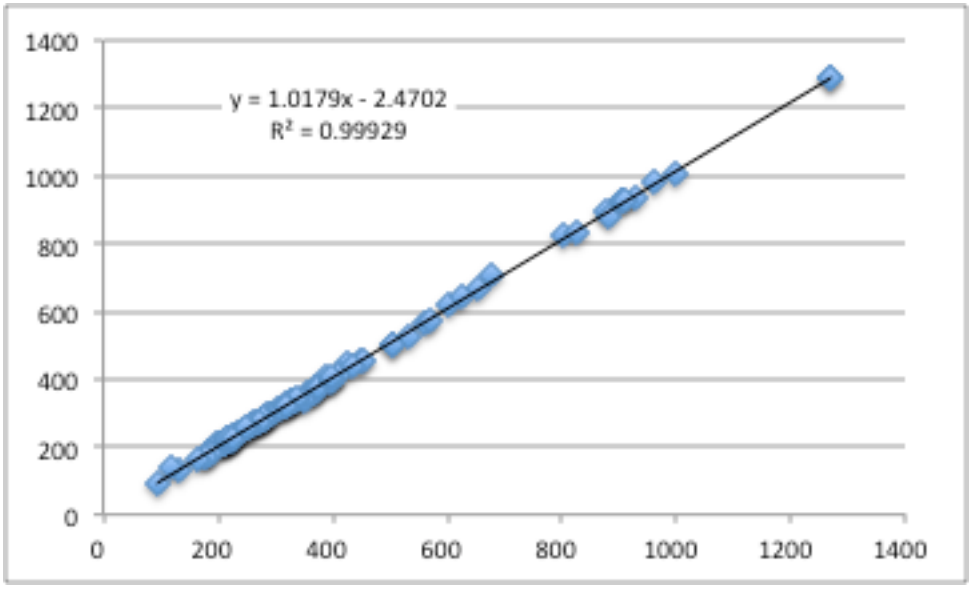

Fig. 1 (a). Same sample Ba abundance (ppm) determined with XRF vs. ICP-MS.

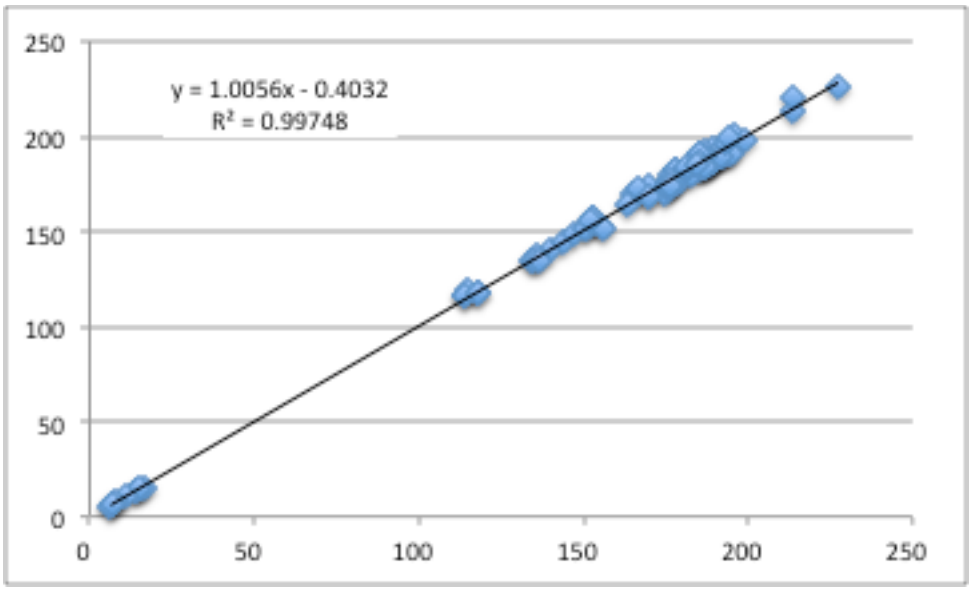

Fig. 1 (b). Same sample Rb abundance (ppm) determined with XRF vs. ICP-MS.

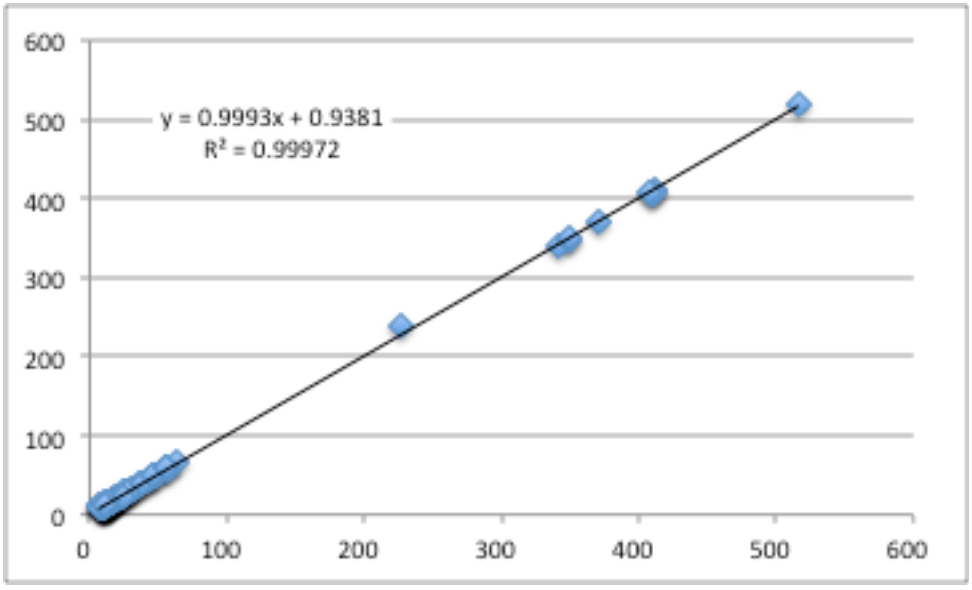

Fig. 1 (c). Same sample Sr abundance (ppm) determined with XRF vs. ICP-MS.

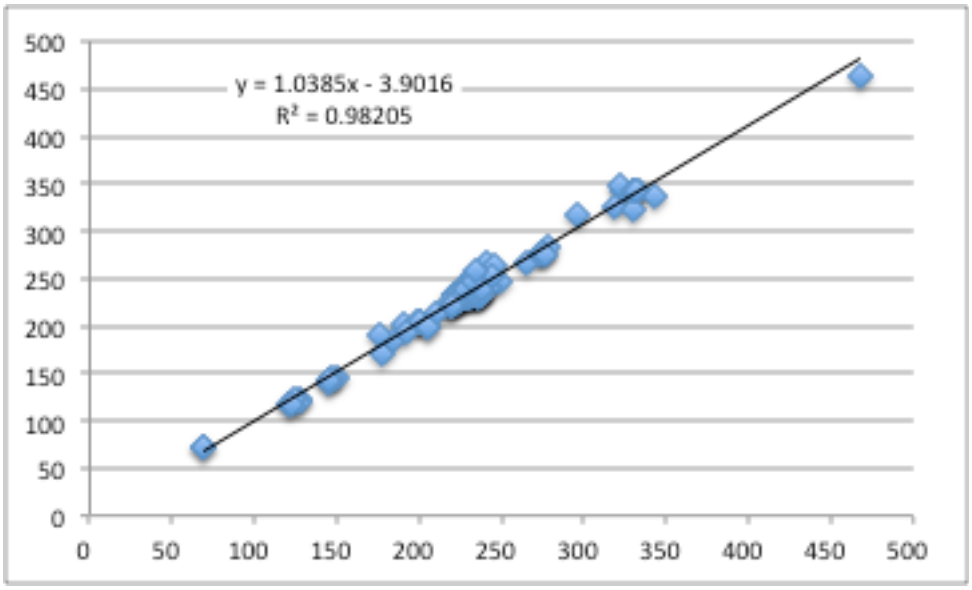

Fig. 1 (d). Same sample Zr abundance (ppm) determined with XRF vs. ICP-MS.

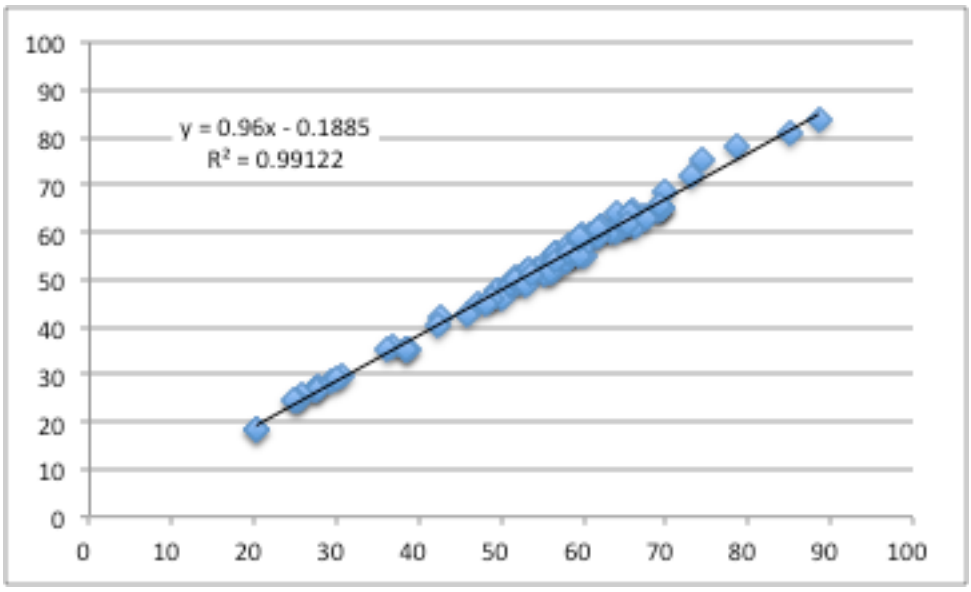

Fig. 1 (e). Same sample Y abundance (ppm) determined with XRF vs. ICP-MS.

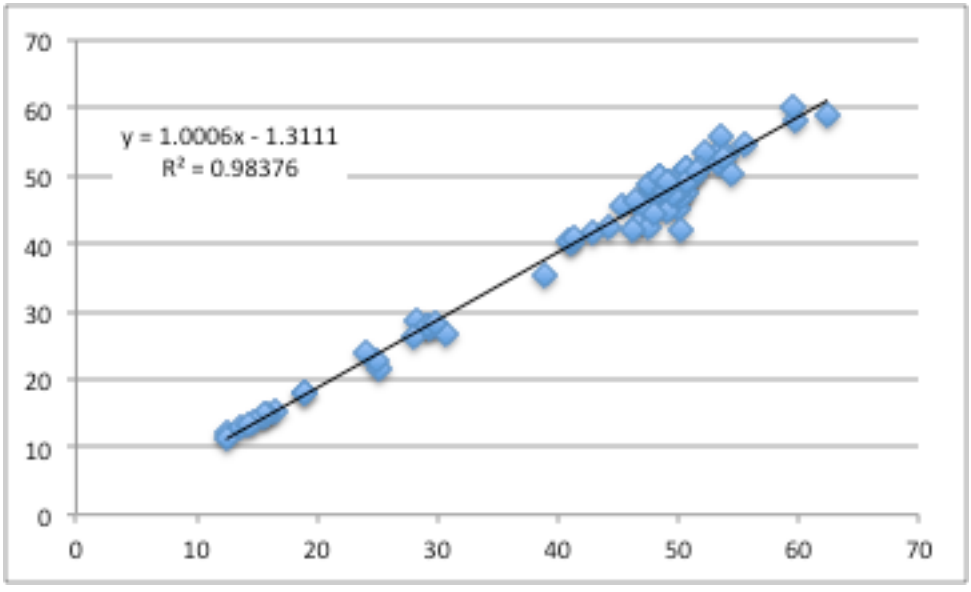

Fig. 1 (f). Same sample Nb abundance (ppm) determined with XRF vs. ICP-MS.

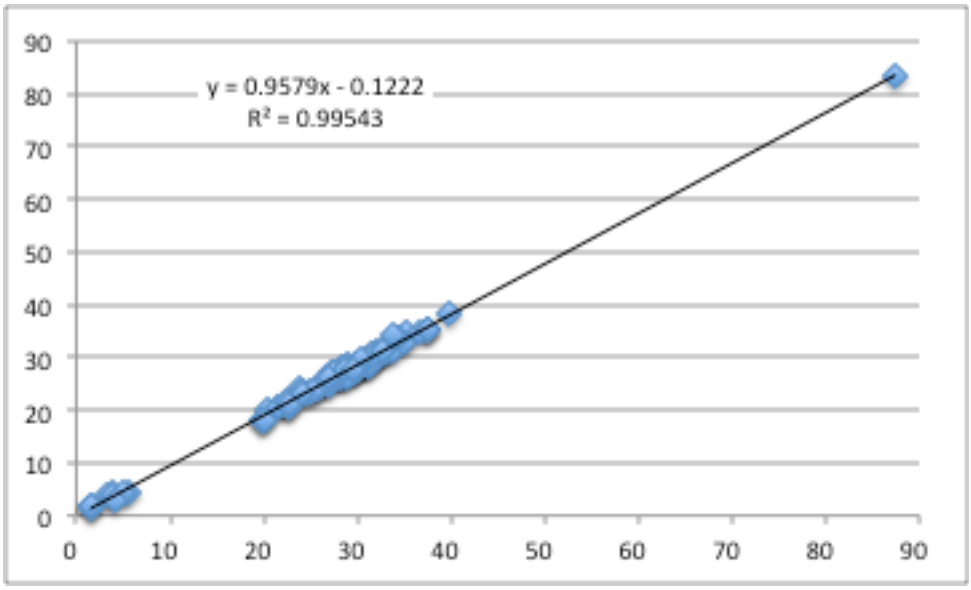

Fig. 1 (g). Same sample Pb abundance (ppm) determined with XRF vs. ICP-MS.

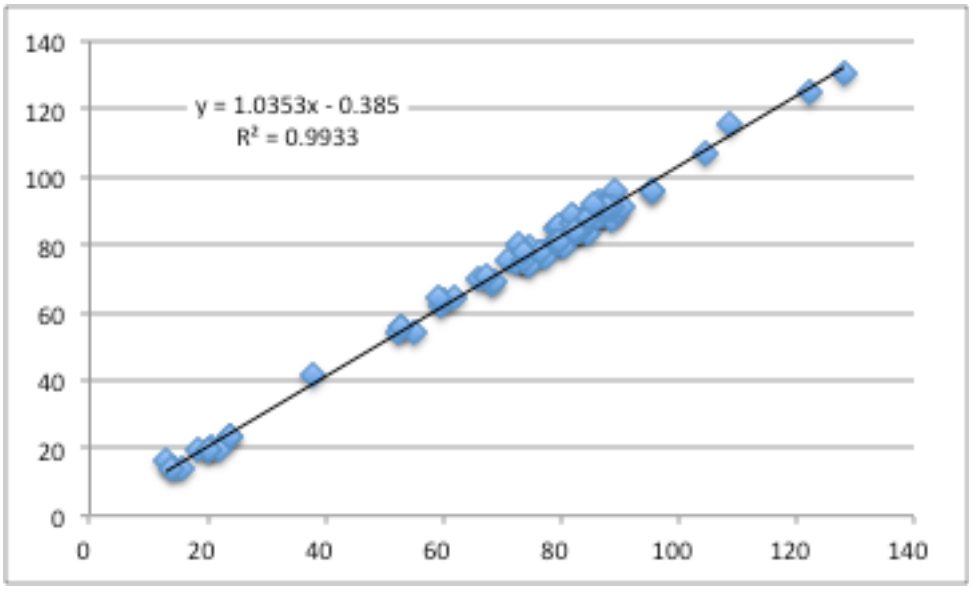

Fig. 1 (h). Same sample La abundance (ppm) determined with XRF vs. ICP-MS.

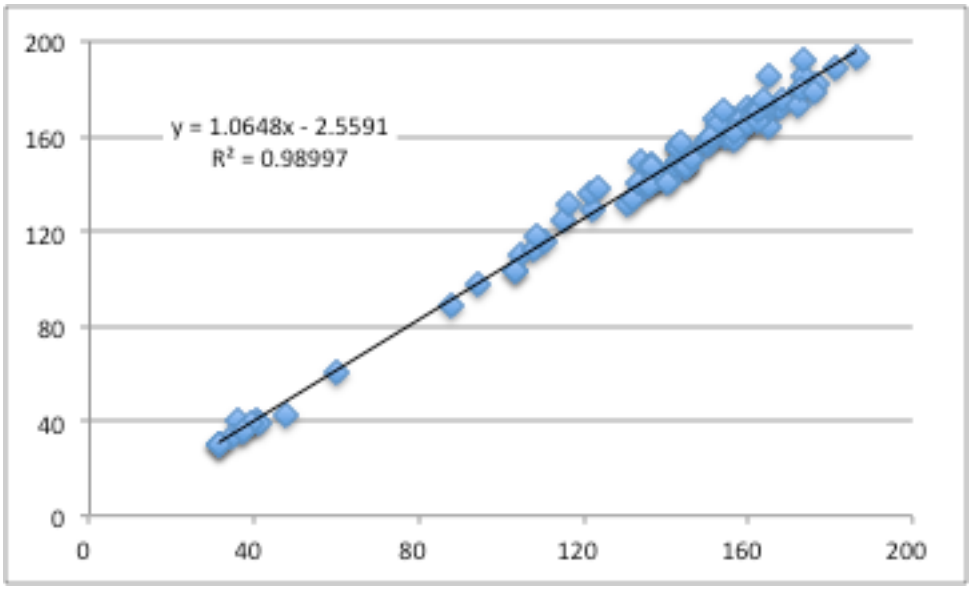

Fig. 1 (i). Same sample Ce abundance (ppm) determined with XRF vs. ICP-MS.

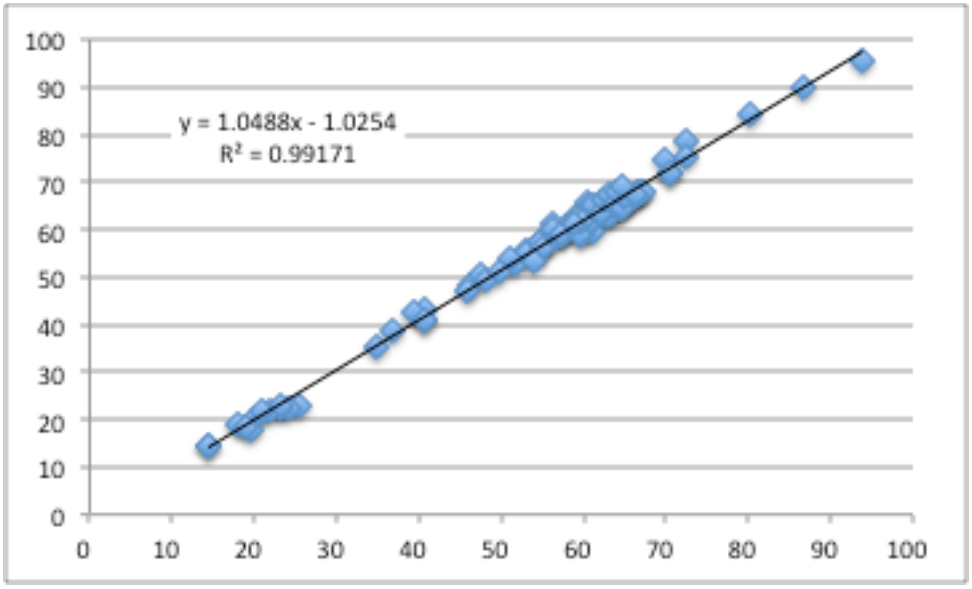

Fig. 1 (j). Same sample Nd abundance (ppm) determined with XRF vs. ICP-MS.

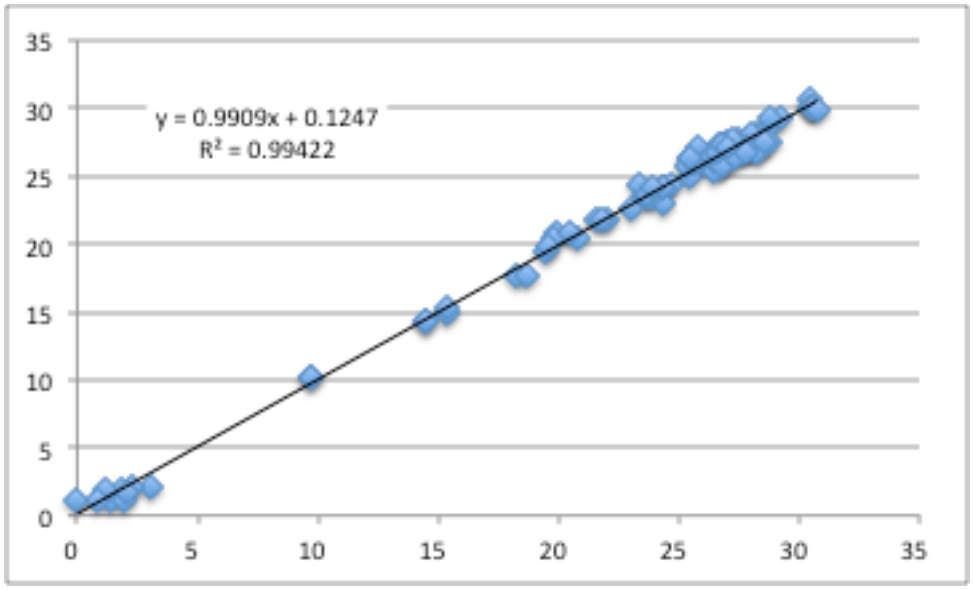

Fig. 1 (k). Same sample Th abundance (ppm) determined with XRF vs. ICP-MS.

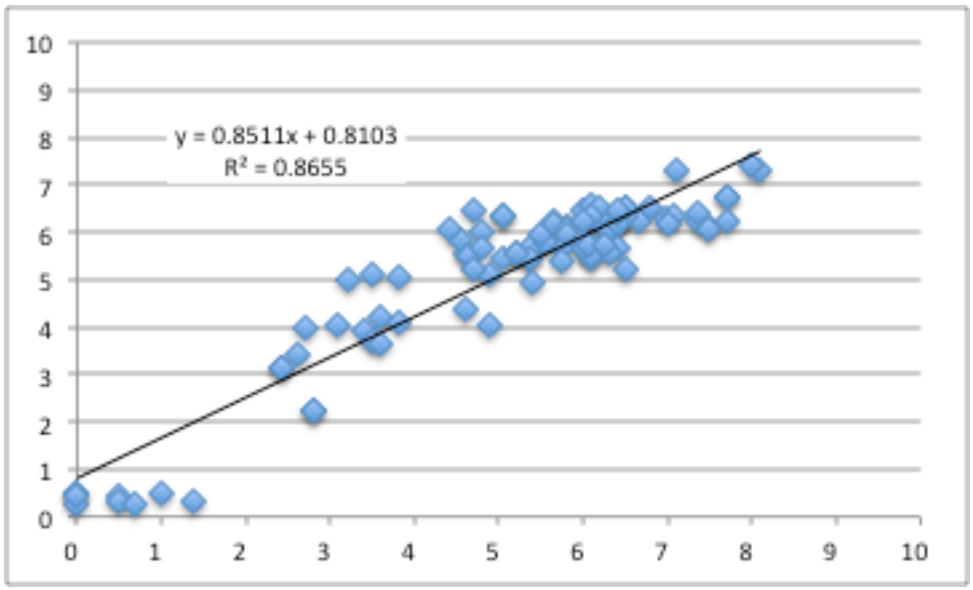

Fig. 1 (l). Same sample U abundance (ppm) determined with XRF vs. ICP-MS.

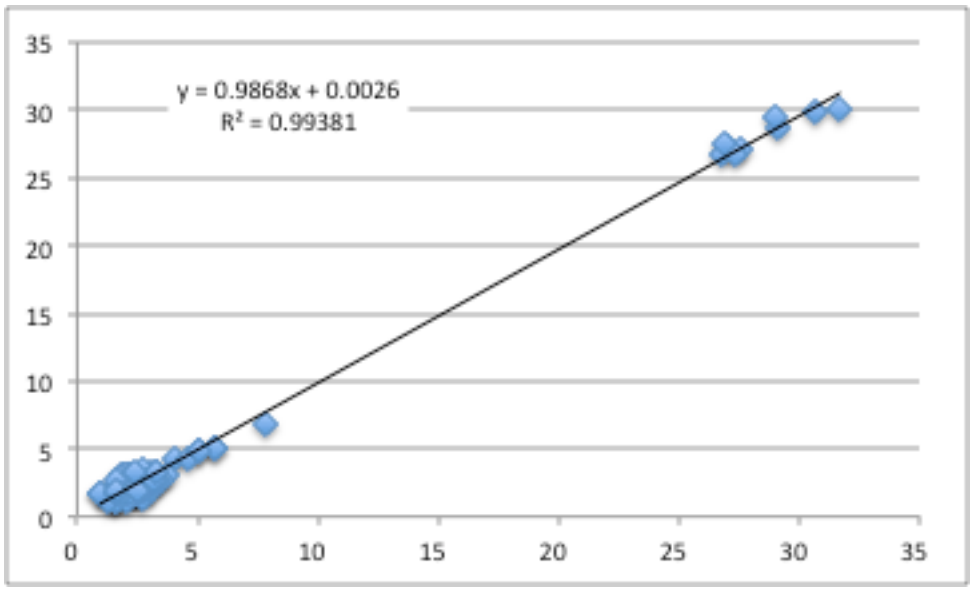

Fig. 1 (m). Same sample Sc abundance (ppm) determined with XRF vs. ICP-MS.

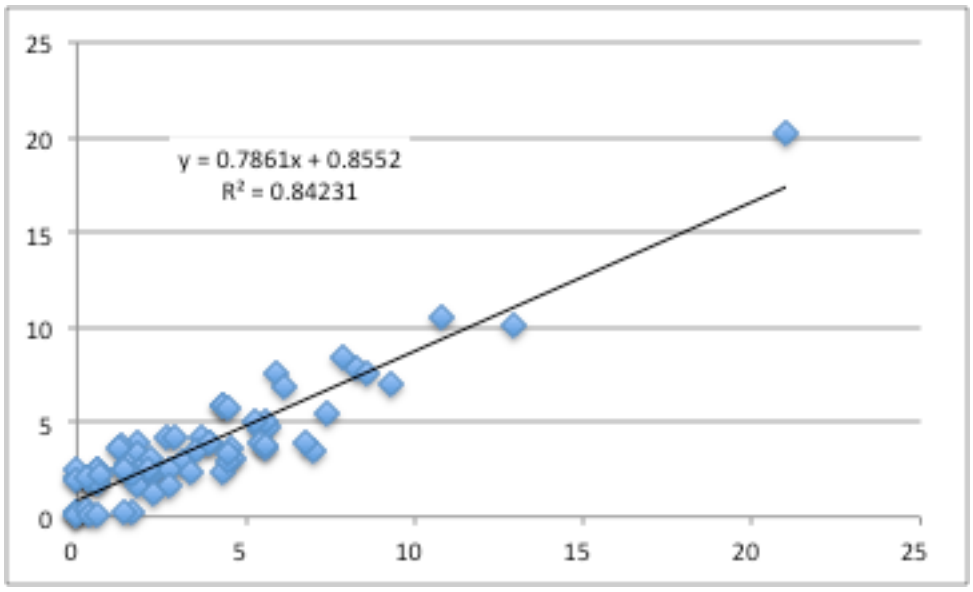

Fig. 1 (n). Same sample Cs abundance (ppm) determined with XRF vs. ICP-MS.

and we repeated two of the analyses with ICP-MS to obtain better agreement with the XRF determined values. The normal sample weights as noted earlier are 3.5 grams for the XRF sub-sample and 2.0 or 3.0 grams for the ICP-MS. For the first set of samples we employed 2.0 grams for the ICP-MS sub-sample but we found that several samples agreed for virtually all elements other than Nb and Ta (Table 2), so we switched to 3.0 grams for the later analyses (but still encountered the problem). Increasing concentration with an increase in sample mass strongly suggests that Nb and Ta are present in a mineral phase that is subject to nugget effects. These effects are common in ores where the mined metal is present in very high concentrations within a sparse mineral phase. Unless an adequate mass of sample is used, analyses of the material will yield low concentrations of the target metal due to lack of entraining any of the sparse parent phase within the sample volume. We suspect the nugget effect in this case is due to the presence of significant chevkinite in the the Lava Creek tuff (Christiansen, 2001). Chevkinite can contain significant concentrations of Nb and Ta (MacDonald et al., 2009) and thus could serve as the nugget phase for both elements. The spread in Nb concentrations at about 50 ppm (Fig. 1f) and the relatively poorer correlation of XRF and ICP-MS Nb abundances compared to other trace elements, testify to the nugget effect for this element in these samples. Larger powdered sample volumes, greater than 3.0 grams, should be employed for trace element analyses of these materials. The presence of a nugget effect between 2.0 to 3.0 and 3.5 grams powder might raise the issue of whether 3.5 grams is sufficient for these samples, but the consistency of Nb concentrations from sample to sample supports the interpretation that 3.5 grams is likely adequate.

Fines fraction samples

We received several samples of fines fractions separated from the coarser chip samples by sieving. Analysis of these fines was confusing, there is only the crudest correlation of elemental concentrations in the fines compared to the coarse chip fractions (Fig. 2). Some samples show equivalent concentrations for some elements (e.g. Zr in Fig. 2b), but most elements are not consistently similar or consistently higher or lower in abundance. The fines fractions are subject to the greatest potential for contamination, possibly including powdered sample from all higher levels in the borehole, so the data for these fines samples appears to be of little use and should be discarded.

Table 2. ICP-MS repeat analyses (values in ppm) with increased sample mass.

	Norris 250-255' 2.0 g	Norris 250-255' 3.5 g	Lava Crk A 2.0 g	Lava Crk A 3.5 g
La	75.40	75.54	77.04	78.99
Ce	113.26	110.25	150.23	148.28
Pr	16.06	16.10	16.43	16.97
Nd	56.85	57.59	57.47	60.21
Sm	12.23	12.39	12.95	13.44
Eu	0.54	0.55	0.41	0.51
Gd	11.24	11.33	12.55	13.28
Tb	1.99	1.98	2.35	2.39
Dy	12.18	12.30	14.79	15.31
Ho	2.44	2.46	3.01	3.08
Er	6.60	6.57	8.11	8.33
Tm	0.98	0.99	1.20	1.21
Yb	5.96	6.07	7.14	7.29
Lu	0.89	0.89	1.04	1.07
Ba	204	207	119	142
Th	27.37	27.23	28.75	29.33
Nb	**45.29**	**53.56**	**46.10**	**60.06**
Y	63.73	63.30	77.16	78.28
Hf	7.59	7.48	7.20	7.54
Ta	**3.25**	**4.09**	**3.27**	**4.31**
U	6.19	6.30	7.16	7.40
Pb	25.72	24.80	24.10	23.96
Rb	197.6	196.4	215.1	220.3
Cs	3.85	3.92	3.54	3.94
Sr	12	15	8	12
Sc	1.5	1.4	1.3	1.6
Zr	196	202	178	190

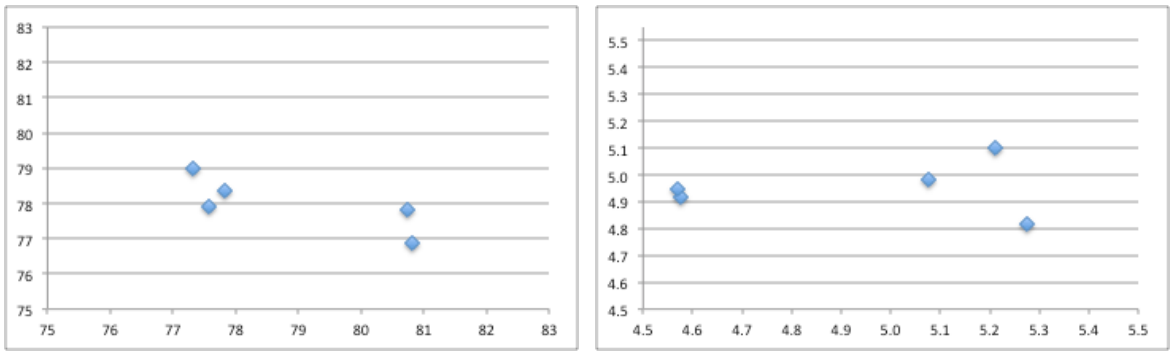

Fig. 2 (a). Normal vs. fines sample determinations for SiO_2 and K_2O (both wt%).

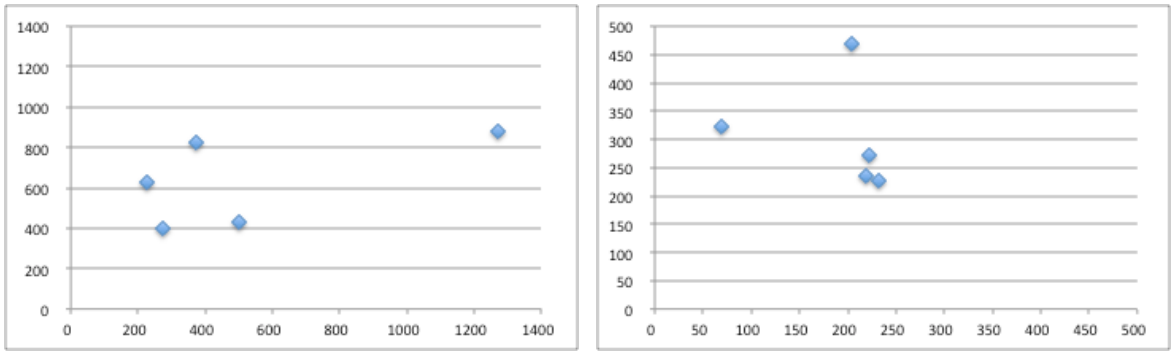

Fig. 2 (b). Normal vs. fines sample determinations for Ba and Zr (both ppm).

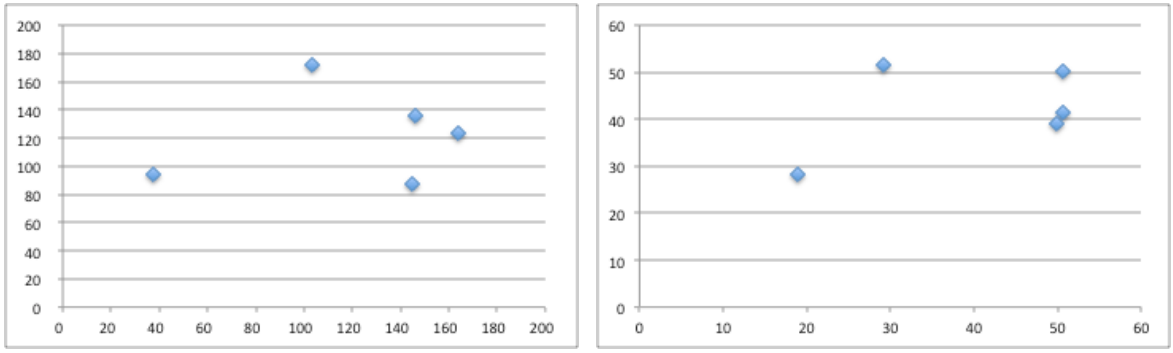

Fig. 2 (c). Normal vs. fines sample determinations for Ce and Nb (both ppm).

Washed vs. Unwashed samples

After sieving, the samples were washed with water to completely remove the fines and other potentially lightly adhering contaminants (Cheryl Jaworowski, pers. Comm., 2011). Analyses of 10 unwashed fractions were made. Two of the samples can be directly compared from the same horizons (Table 3) and they suggest there is little significant difference between washed and unwashed material. The remaining unwashed samples are from horizons very close to washed analyzed horizons and in all cases are very similar to their nearest neighbors. Thus the washing did not remove analytically significant amounts of material, and the results from the unwashed samples may be used to amplify the analytical data from the boreholes.

Comments on specific boreholes

The overall similarity of many of these high silica rhyolite analyses render discrimination of the different stratigraphic units problematical based solely upon the geochemical data. As noted above, more credence should be given to log observations, for example of unit contacts, than reliance solely upon geochemical data for stratigraphic correlation. Thus here I can only offer the most general of remarks concerning the stratigraphic implications of these data, and warn the reader that I am not very familiar with the geology and stratigraphy of YNP.

B205 – Norris. The upper part of this hole may include three rhyolite lavas as suggested by the diversity in compositions. The "peach mud" analyzed at 290 feet is similar to the underlying tuff analyses and thus likely derived chiefly from the tuff by reworking or other means. There are subtle but consistent differences between the tuff analyses from 335 to 410 feet compared with the samples from the lower part of the hole, thus there is evidence for the presence of both members of the Lava Creek Tuff.

B206 – Canyon. Rhyolite lava in the upper part of this hole is quite distinct from that lower in the hole. There is no discernable difference between the samples from 165 and 400 feet. An unwashed sample from 395 feet is very similar to the 400 foot sample.

B207 – Madison. The analyzed samples from this hole are all very similar high silica rhyolite, thus the geochemistry is of little use in the interpretation of the stratigraphy. Very subtle changes need to be viewed with the knowledge of sampling and analytical uncertainties firmly in mind.

Table 3. Washed versus unwashed cuttings.

	Grant I 55-60	Grant I 55-60	Norris 190-195	Norris 190-195
Date	13-Aug-12	5-Mar-14	13-Aug-12	5-Mar-14
	washed	unwashed	washed	unwashed
Unnormalized Major Elements (Weight %):				
SiO2	74.27	73.23	75.51	75.83
TiO2	0.158	0.172	0.185	0.184
Al2O3	11.54	11.89	11.97	12.03
FeO*	1.26	1.41	1.89	1.85
MnO	0.027	0.030	0.037	0.036
MgO	0.08	0.15	0.03	0.05
CaO	0.50	0.58	0.69	0.71
Na2O	2.53	2.41	3.56	3.59
K2O	4.69	4.61	4.80	4.79
P2O5	0.013	0.016	0.015	0.015
Sum	95.07	94.49	98.69	99.08
LOI (%)	4.13	3.99	0.76	0.76
Normalized Major Elements (Weight %):				
SiO2	78.12	77.50	76.52	76.53
TiO2	0.167	0.182	0.187	0.186
Al2O3	12.13	12.59	12.13	12.14
FeO*	1.33	1.49	1.91	1.87
MnO	0.028	0.031	0.038	0.037
MgO	0.09	0.16	0.03	0.05
CaO	0.53	0.62	0.70	0.71
Na2O	2.66	2.55	3.61	3.62
K2O	4.94	4.87	4.86	4.83
P2O5	0.014	0.017	0.015	0.015
Total	100.00	100.00	100.00	100.00
Unnormalized Trace Elements (ppm):				
Ni	3	2	2	2
Cr	4	5	3	2
Sc	2	3	3	3
V	4	4	5	5
Ba	427	398	960	998
Rb	196	199	136	136
Sr	19	20	45	47
Zr	221	237	334	330
Y	60	62	57	57
Nb	45.4	46.5	30.6	29.9
Ga	20	21	20	22
Cu	2	2	2	1
Zn	55	59	84	84
Pb	35	37	28	27
La	81	82	73	74
Ce	152	151	143	141
Th	25	27	20	20
Nd	59	59	58	60
U	4	6	4	3
Cs	8	8	4	3
As >/=		3		3
sum tr.	1422	1431	2010	2045
in %	0.14	0.14	0.20	0.20
sum m+tr	95.21	94.64	98.89	99.28
/l+Toxides	95.24	94.67	98.93	99.32
w/LOI	99.37	98.66	99.68	100.08
if Fe3+	99.51	98.82	99.89	100.28
ICP-MS data (ppm)				
La	84.80	84.24	76.21	75.12
Ce	167.08	159.66	149.51	140.29
Pr	17.65	17.72	16.30	15.98
Nd	62.53	62.08	60.67	58.78
Sm	12.14	12.22	12.39	12.12
Eu	0.90	0.85	1.64	1.68
Gd	10.85	10.62	11.29	11.06
Tb	1.85	1.81	1.86	1.82
Dy	11.37	11.25	11.03	10.77
Ho	2.27	2.23	2.19	2.13
Er	6.14	6.09	5.74	5.53
Tm	0.91	0.90	0.82	0.79
Yb	5.61	5.54	4.86	4.81
Lu	0.82	0.84	0.73	0.70
Ba	443	403	985	1006
Th	25.82	26.27	20.37	19.83
Nb	45.66	46.21	26.56	28.27
Y	59.29	58.64	55.38	53.60
Hf	8.01	8.22	10.29	9.73
Ta	3.34	3.34	1.72	1.90
U	6.07	5.86	4.12	4.03
Pb	34.53	34.81	26.39	26.00
Rb	200.5	198.5	137.1	134.9
Cs	7.89	8.44	2.36	2.28
Sr	22	21	49	49
Sc	2.4	2.7	2.0	1.9
Zr	232	237	342	324

B208 – Lake. Similar to the Madison borehole, the high-silica rhyolites in the middle and lower portions of this hole are difficult to discriminate solely upon their geochemistry. The rhyolite near the base of the hole is quite distinct, and appears to be quite altered based upon its too high silica content. Sediment at the top and bottom of the hole is distinct from the rhyolites. One unwashed sample from 490 feet is very similar to a washed sample from 510 feet.

Grant I. The two uppermost samples in this hole are weathered or altered, while the lower part of the hole is consistent and fairly fresh high-silica rhyolite.

B944 – Grant II. A "chaotic tuff" at 260 feet is very distinct chemically. It separates two packages of high-silica rhyolites that are again only subtly different in composition. An unwashed sample of the chaotic tuff is very similar to its washed counterpart. An unwashed rhyolite at 240 feet is similar to the rhyolites in the upper part of the hole.

B945 – Panther Creek. This borehole penetrated a significant thickness of basalt and encountered rhyolite only at the bottom. An unwashed sample of the basalt from 290 feet is essentially identical to a washed sample at 240 feet.

Negative Ce anomalies in REE profiles

The majority of the borehole samples have smooth REE patterns with the exception of the prominent negative Eu anomalies expected in high-silica rhyolite. Eu is the sole REE that can adopt +2 valence, and in that reduced form is highly compatible in plagioclase and sanidine during the growth of those two minerals in magmas. Small, barely significant negative Ce anomalies are present in samples from most of the boreholes. The exception is the Norris borehole, where the majority of samples below 120 feet have prominent negative Ce anomalies. Ce can be fractionated from the remaining REEs in oxidized hydrothermal environments due the fact that Ce is the sole REE that can adopt +4 valence under oxidizing conditions. Ce^{+4} is easily mobilized by carbonic acid and perhaps other ligands and anions. Study of the hydrothermal alteration present in older boreholes in the Norris basin indicates that REE-bearing minerals were in part dissolved by hydrothermal fluids and the REEs redistributed nearby by condensation from the fluids (White et al., 1988). Such processes could well have resulted in fractionation of Ce from the other REEs and thus in Ce anomalies.

Acknowledgements: Laureen Wagoner, Scott Boroughs, and Charles Knaack of the Peter Hooper GeoAnalytical Laboratory were responsible, along with the author, for overall direction of sample preparation and analysis. Sample preparation was performed by several undergraduates including Daniel Verrel, Kellie Wall, Camden Nix, Cameron Mercer, Alayne Donnelly, Julianna Dippold, Matt Risner, and Betsy Scarborough. Stratigraphic advice for the YNP area was kindly provided by Jennifer Staffenberg, currently a graduate student at WSU.

References cited

Christiansen, R.L., 2001, The Quaternary and Pliocene Yellowstone Plateau Volcanic Field of Wyoming, Idaho and Montana: USGS Prof. Paper 729-G.

Jaworowski et al., in progress, Physical Results of Borehole Strainmeter Drilling in Yellowstone National Park, 2007 and 2008, Yellowstone National Park, Wyoming.

Johnson, D.M., Hooper P.R., and Conrey, R.M., 1999, XRF Analysis of Rocks and Minerals for Major and Trace Elements on a Single Low Dilution Li-tetraborate Fused Bead, Advances in X-ray Analysis, 41: 843-867.

Macdonald, R.; Belkin, H. E.; Wall, F.; Baginski, B., 2009, Compositional variation in the chevkinite group: New data from igneous and metamorphic rocks: Mineralogical Magazine, 73: 777 – 796.

White. D.E., Hutchinson, R.A., and Keith, T.E.C., 1988, The Geology and Remarkable Thermal Activity of Norris Geyser Basin, Yellowstone National Park, Wyoming: USGS Prof. Paper 1456.